Supporting Text

Effects of Prior Distribution of R_0

We examined the effects of the prior on R_0 in three ways. First, we recalculated the posterior distribution under three additional prior scenarios on R_0: (*i*) a grave scenario, with the prior median of R_0 set to a relatively high value of 15.4; (*ii*) an optimistic scenario, with the prior median of R_0 set to a relatively low value of 1.8; and (*iii*) a pessimistic scenario with the prior median of R_0 set to a moderately high value of 7 (Table 2). The median values of the optimistic and pessimistic prior distributions reflect the low and high values of R_0 assumed in a previous model of smallpox (1). An important observation is that the curvature of the prior tails is important for the length of the posterior tails and, consequently, for the reported credible intervals (CIs). Although the posterior point estimates and CIs consequently differ somewhat among the four sets of prior scenarios, the comparison between the two intervention strategies nevertheless remains essentially unchanged. Mass vaccination is always favored over trace vaccination regardless of the prior distribution on R_0. All other parameters' prior distributions purposefully were made informative based on the available literature, and, thus, we did not explore the sensitivity to those priors.

The changes in the posterior estimates of R_0 as the prior changed were roughly what one would expect (Table 2 and Fig. 4). In particular, there was considerable overlap across estimates of the posterior. For Old World populations, the median value of the estimate shifted only under the pessimistic prior, which was a result of this prior being much narrower than the other priors under consideration (Fig. 4*C*). For New World populations, the median values were similar except under the optimistic prior (Fig. 4*B*), for which the median of the distribution was higher. The shift to larger values under the optimistic prior occurred because the tail of the log-normal prior on R_0 is essentially flat in the region for which the likelihood is also flat. At higher values of R_0, it therefore becomes increasingly difficult to differentiate between likely draws of R_0 under the Markov chain Monte Carlo (MCMC) sampler, as in Fig. 1. The long tail on the posterior reflects this lack of

information. In fact, strictly speaking, this prior is not truly optimistic, because it assigns substantial probabilities to high values of R_0.

We also considered the effect of varying speeds of diagnosis on the optimal vaccination strategy. Specifically, we considered the effect of allowing diagnosis to occur when macales appear versus when pustules appear (see *Variability in the Parameters of the Vaccination Model* for further information about the stages of smallpox). This change had no effect on the percentage of draws from the MCMC sampler that favored mass vaccination. Changes in the priors similarly had little effect (Figs. 5-7). Finally, we compared our results to the results of Gani and Leach (2) by assuming, as they did, that there is no uncertainty in any parameters except R_0 and σ, by fixing the remaining parameters at the same values that they used, and by using in our likelihood calculation the same epidemic data sets that they used. Under these assumptions, the median value of R_0 that Gani and Leach (2) report is very close to the median value of our posterior distribution. Additionally, the range of Gani and Leach's (2) R_0 values for smallpox is centered within the 35th to 60th percentile of our posterior distribution.

$\mathbf{R_0}$ Estimates and Model Fit

To show the fit of the susceptible-exposed-infected-recovered (SEIR) model to the epidemic data, we simulated a series of epidemic curves by using the median and the 95% CI for R_0 and the median posterior estimates of the other disease parameters (Table 1), and we plotted the resulting model predictions against four of the epidemic data sets. In interpreting the result, note that we are fitting a common value of R_0 to multiple epidemic data sets. Although fitting population-specific values of R_0 to each epidemic would provide a better fit, doing so very likely would increase the overall uncertainty in R_0, reemphasizing our main point. Given this caveat, Fig. 8 shows that the 95% CIs for R_0 include most of the data, and the predictions based on the median value are also close to the data. The model fits for the other epidemics, which are not shown, are similar in appearance.

Fig. 4. Effects of changes in the prior distribution (solid line) on the posterior histogram of R_0 for Old-World (A,C, and E) and New-World (B,D, and F) populations. (A) and (B) are for an optimistic scenario with a median of 1.8, (C) and (D) are for a grave scenario with a median of 15.4, and (E) and (F) are for a pessimistic scenario with a median of $R_0 = 7$. Note changes in scale.

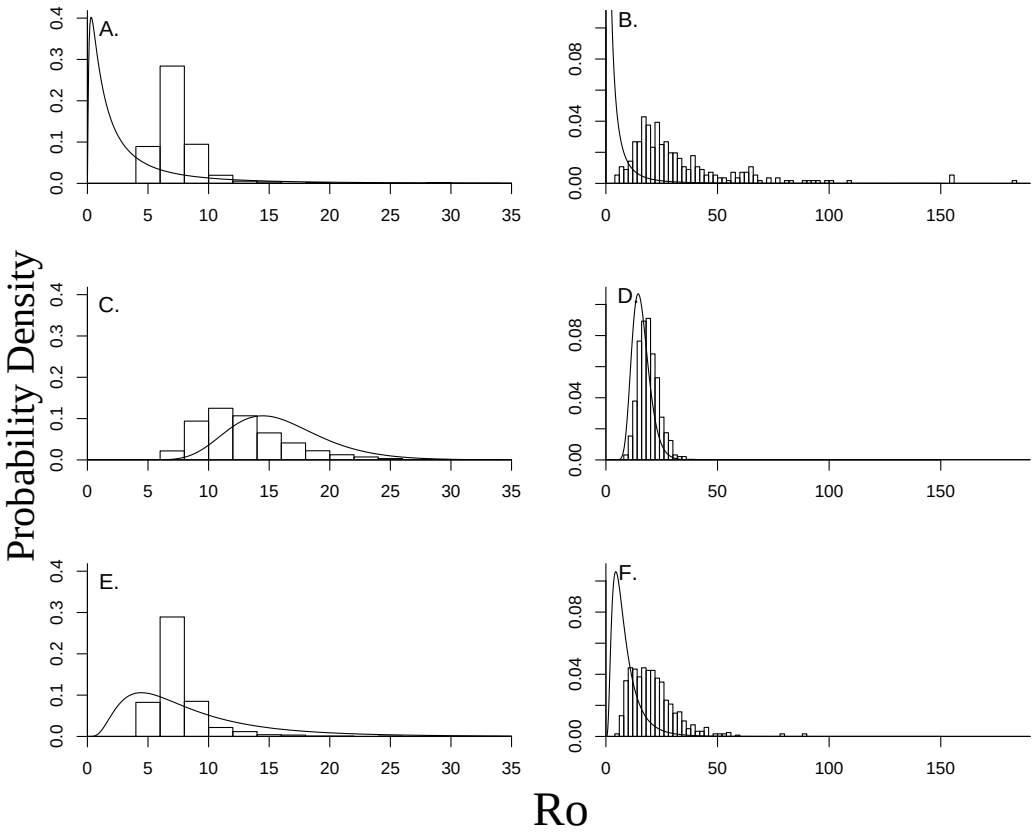

Fig. 5. Difference in the number of fatalities using trace vaccination rather than mass vaccination for Old-World (A and C) and New-World (B and D) populations. In (A) and (B), diagnosis occurs after macales, while in (C) and (D) diagnosis occurs only after pustules appear. All cases assume an optimistic prior distribution on R_0. Note changes in scale.

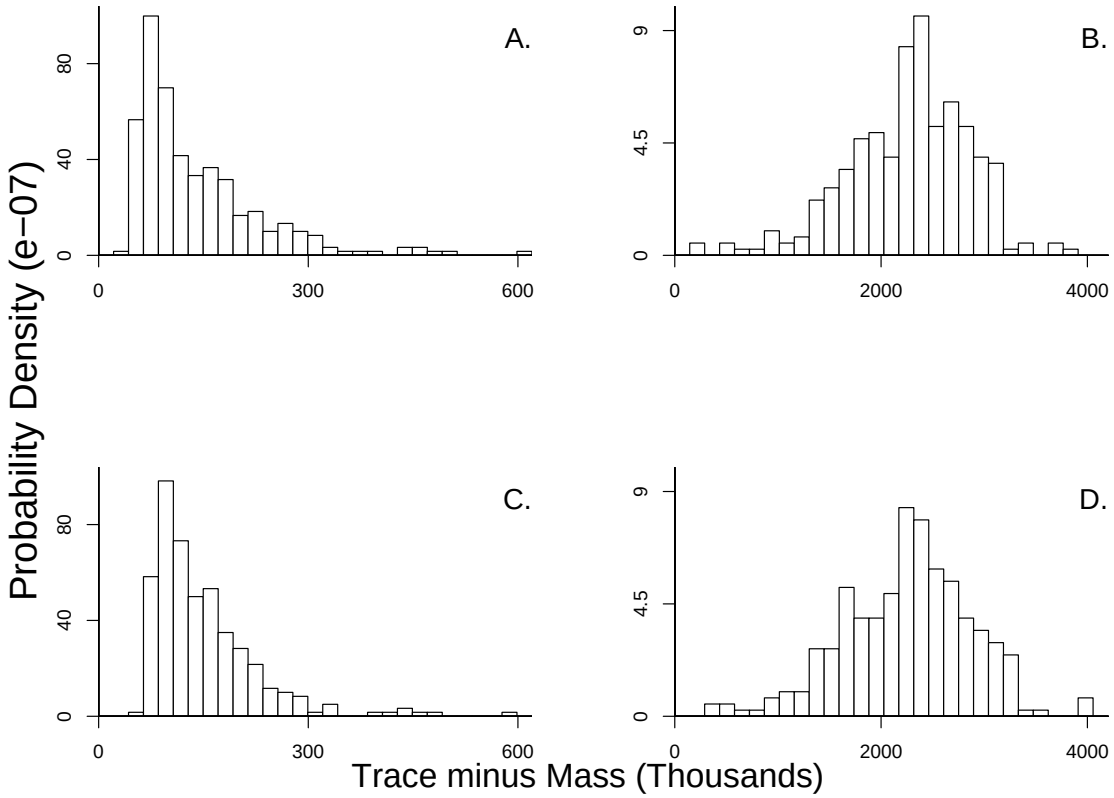

Fig. 6. As in Fig. 5, but for a grave prior distribution, such that the median on $R_0 = 15.4$.

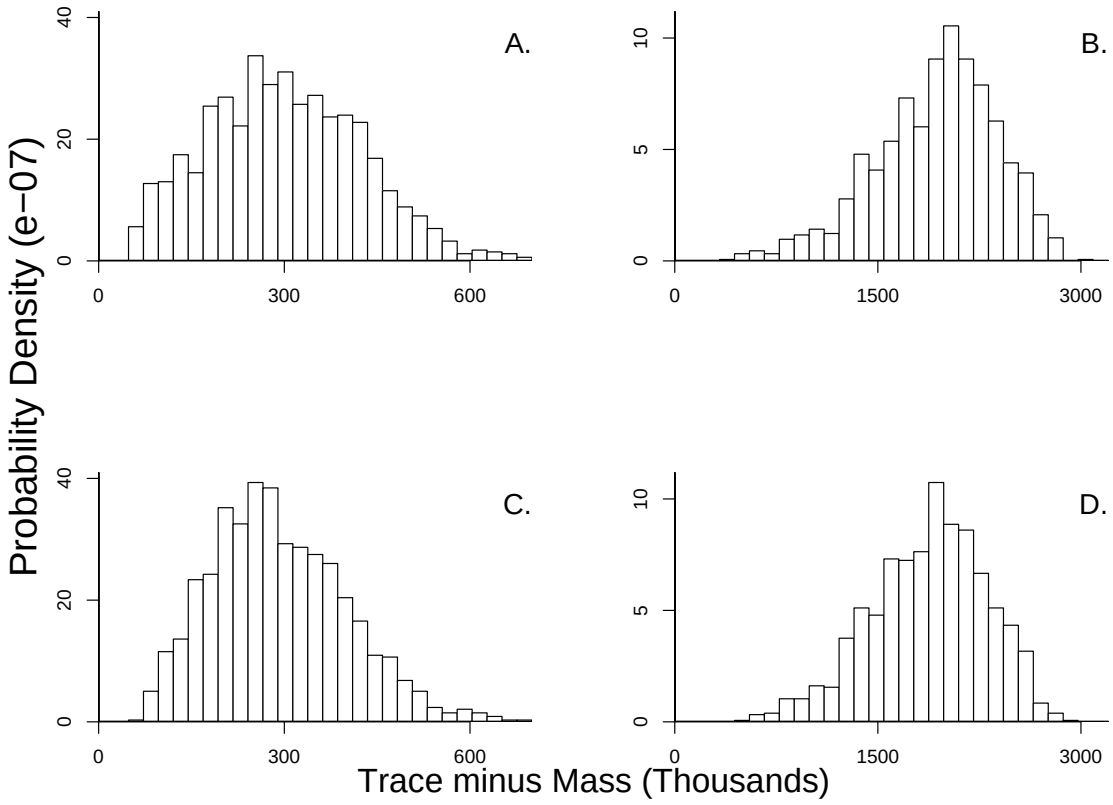

Fig. 7. As in Fig. 5, but for a pessimistic prior distribution, such that the median on $R_0 = 7$.

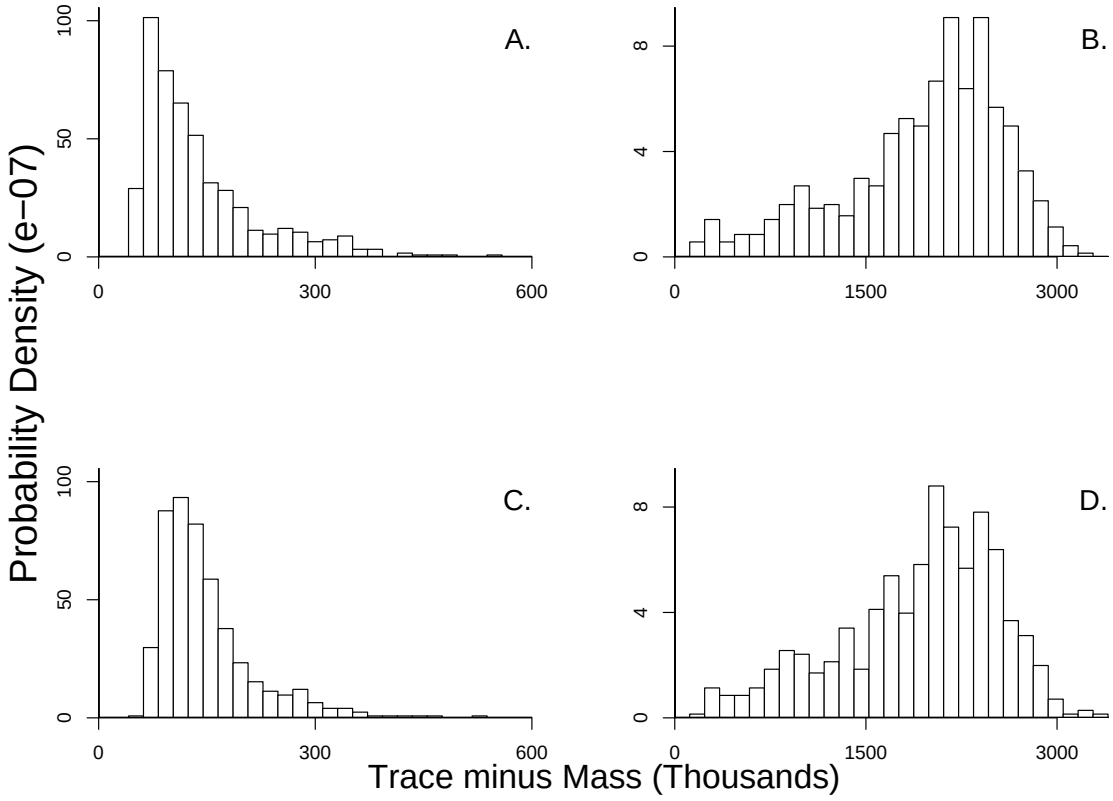

Table 2. Sensitivity of prior estimates of R_0 (with 95% CI) to the median posterior value of R_0 (with 95% CI).

Estimate	Prior	Posterior
Original – New World	4 (0.7, 23.7)	7.1 (5.0, 15.3)
Old World		17.5 (5.9, 59.5)
Optimistic – New World	1.8 (0.13, 24.2)	7.1 (5.3, 12.2)
Old World		26.9 (9.5, 88.4)
Grave – New World	15.4 (9.4, 25.1)	12.1 (7.5, 21.7)
Old World		18.6 (11.7, 29.2)
Pessimistic – New World	7 (1.9, 26.3)	6.9 (5.3, 12.8)
Old World		19.2 (7.7, 45.5)

Advantages of a Bayesian Approach

The Bayesian approach that we use allows us to incorporate information from as many data sets as possible, including both hospital data on smallpox progression and multiple historical epidemics. Although non-Bayesian methods such as a bootstrap of parameter values (3) may be able to incorporate certain features of this analysis, such methods most likely would fail to account for any potential nonnormality or multimodality of the posterior distribution.

An additional advantage of a Bayesian approach comes from its ability to take true expert opinion into account when establishing prior distributions regarding potentially unknown parameters. For example, we relied on informed expert opinion to center the distribution of mortality rates for Old World populations (4) and, thus, to combine the mortality data coherently with the likelihood. Given these issues, the Bayesian framework represents a particularly promising approach for combining disparate information, expert opinion, and multiple data sets when estimating the parameters of epidemic models.

Fig. 8. Estimates of epidemic trajectories in two Old-World (A and B) and two New-World (C and D) populations. The triangles represent the data from the individual epidemics. The solid line was constructed using the median value of R_0 from the posterior estimate. The dashed lines were constructed using the upper and lower 95% CI of R_0. The populations used in constructing the figure were Boston, Warrington, Santa Clara, and Saint Lawrence (see Table 3), respectively.

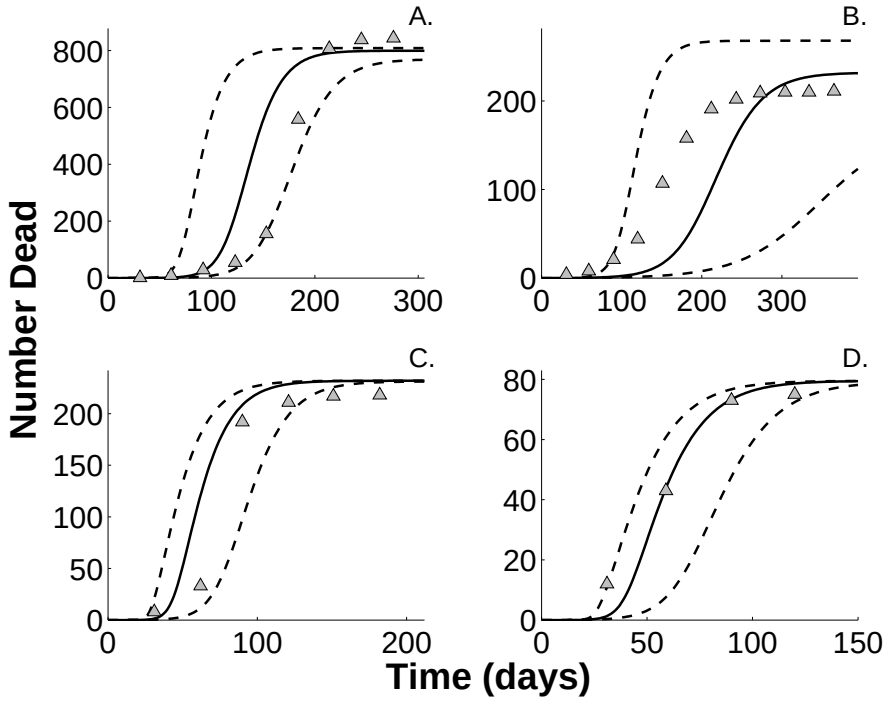

The Vaccination Model

In order to translate the uncertainty in the posterior distribution of the SEIR parameters into uncertainty regarding the best vaccination strategy, we used a general queuing model proposed by Kaplan *et al*. (5). This model is composed of a suite of ordinary differential equations (ODEs) that group individuals into one of five states. These states comprise untraced individuals, individuals who are in the queue to receive a vaccination, individuals who are quarantined, individuals who are successfully traced but unsuccessfully vaccinated, and individuals who are either recovered/immune or dead. By following Kaplan *et al*.'s (5) notation, the equations take the following form:

Untraced Individuals –

$$\frac{dS^0}{dt} = -\beta I_3 S^0 - [c - pR_0(t)]\,\frac{S^0}{N} r_3 I_3 \tag{4}$$

$$\frac{dI_1^0}{dt} = \beta I_3 S^0 - \left\{[c - pR_0(t)]\,\frac{I_1^0}{N} + p\lambda_1(t)\right\} r_3 I_3 - r_1 I_1^0 \tag{5}$$

$$\frac{dI_2^0}{dt} = r_1 I_1^0 - \left\{[c - pR_0(t)]\,\frac{I_2^0}{N} + p\lambda_2(t)\right\} r_3 I_3 - r_2 I_2^0 \tag{6}$$

$$\frac{dI_3^0}{dt} = r_2 I_2^0 - \left\{[c - pR_0(t)]\,\frac{I_3^0}{N} + p\lambda_3(t)\right\} r_3 I_3 - r_3 I_3^0 \tag{7}$$

$$\frac{dI_4^0}{dt} = r_3 I_3^0 - r_4 I_4^0 \tag{8}$$

The superscript 0 represents untraced individuals, as opposed to the superscript of 1 that represents traced individuals (See Eqs. **14**-**18**). S^0 denotes the number of untraced susceptibles and I_j^0 denotes the number of untraced infected individuals in infected disease stage j. The disease stages are then as follows: $j = 1$ indicates noninfectious individuals who are showing no symptoms and who are vaccine-sensitive; $j = 2$ indicates noninfectious individuals who are also showing no symptoms but who are vaccine-*in*sensitive; $j = 3$ indicates individuals who are showing no symptoms but who are infectious; finally, $j = 4$ indicates individuals who are showing symptoms and who have therefore been isolated. I_3 is composed of the sum of $I_3^0 + I_3^1 + Q_3$, where Q_3 denotes the number of individuals in the queue who are in disease stage 3. In the above equations and those that follow, c represents the number of contacts named per infected individual, and p is the fraction of infected contacts who have been named. N denotes the overall population size, and r_j represents the rate at which individuals stay in disease stage j. Lastly, $\lambda_j(t)$ is the expected number of untraced contacts at time t and disease stage j, whereas $R_0(t)$ is the reproductive rate of spread of the disease at time t.

The time at which asymptomatic individuals enter the queue, whether they are susceptible or infected, depends upon the vaccination strategy. Under mass vaccination, all individuals enter the queue to be vaccinated when an outbreak occurs. Under trace vaccination, only individuals who

have been named by an infected individual enter the queue to be vaccinated. For individuals in the queue to be vaccinated, the equations comprise:

Queued Individuals –

$$\frac{dQ_0}{dt} = [c - pR_0(t)]\,\frac{S^0}{N} r_3 I_3 - \beta I_3 Q_0 - \mu Q_0 min(1, n/Q) \quad (9)$$

$$\frac{dQ_1}{dt} = \beta I_3 Q_0 + \left\{[c - pR_0(t)]\,\frac{I_1^0}{N} + p\lambda_1(t)\right\} r_3 I_3 - \mu Q_1 min(1, n/Q) - r_1 Q_1 \quad (10)$$

$$\frac{dQ_2}{dt} = r_1 Q_1 + \left\{[c - pR_0(t)]\,\frac{I_2^0}{N} + p\lambda_2(t)\right\} r_3 I_3 - \mu Q_2 min(1, n/Q) - r_2 Q_2 \quad (11)$$

$$\frac{dQ_3}{dt} = r_2 Q_2 + \left\{[c - pR_0(t)]\,\frac{I_3^0}{N} + p\lambda_3(t)\right\} r_3 I_3 - \mu Q_3 min(1, n/Q) - r_3 Q_3 \quad (12)$$

Here Q_j represents the number of individuals that are currently in the queue, with j again representing the stage of the disease that they are in. The speed at which individuals cycle through the queue is determined by the number of tracers/vaccinators n, and the rate at which individuals in the queue are found and vaccinated μ. Given that there is a fixed number of individuals who are able to trace and/or vaccinate, there is a maximum number of individuals that can be removed from the queue. This number is determined by $min(1, n/Q)$, where $Q = \sum_{j=1}^{3} Q_j$.

Febrile individuals are also subject to quarantine if identified. The equation describing their dynamics takes the form,

Quarantined Individuals –

$$\frac{dH}{dt} = (1 - f)h\mu Q_3 min(1, n/Q) - r_3 H - \alpha H. \quad (13)$$

Here, H represents the number of quarantined individuals who are febrile. h denotes the fraction of individuals who are febrile and in stage 3, f is the vaccination fatality rate, and α is the rate at which febrile individuals are vaccinated.

The equations for the number of individuals who are successfully traced but unsuccessfully vaccinated are as follows.

Traced but Unsuccessfully Vaccinated Individuals –

$$\frac{dS^1}{dt} = (1-f)(1-\nu_0)\mu Q_0 min(1, n/Q) - \beta S^1 I_3 \quad (14)$$

$$\frac{dI_1^1}{dt} = \beta S^1 I_3 + (1-f)(1-\nu_1)\mu Q_1 min(1, n/Q) - r_1 I_1^1 \quad (15)$$

$$\frac{dI_2^1}{dt} = r_1 I_1^1 + (1-f)\mu Q_2 min(1, n/Q) - r_2 I_2^1 \quad (16)$$

$$\frac{dI_3^1}{dt} = r_2 I_2^1 + (1-f)(1-h)\mu Q_3 min(1, n/Q) + \alpha H - r_3 I_3^1 \quad (17)$$

$$\frac{dI_4^1}{dt} = r_3(I_3^1 + Q_3 + H) - r_4 I_4^1 \quad (18)$$

Here, ν_j is the vaccine efficacy for stage j, and a superscript of 1 denotes individuals who have been traced but unsuccessfully vaccinated, as previously noted.

The final two equations track the number of recovered-and-immune individuals and the number of dead. These equations take the following form.

Recovered-and-Immune and Dead Individuals –

$$\frac{dZ}{dt} = (1-f)(\nu_0 Q_0 + \nu_1 Q_1)\mu \, min(1, n/Q) + (1-\delta) r_4 (I_4^0 + I_4^1) \quad (19)$$

$$\frac{dD}{dt} = f\mu Q \, min(1, n/Q) + \delta r_4 (I_4^0 + I_4^1) \quad (20)$$

Here, Z and D represent the number of immune/recovered individuals and the number of dead, respectively. δ is the death rate for smallpox.

In our analyses, all values derived from the multivariate draws of the posterior are placed into the above ODEs and used to determine the number that die under trace versus mass vaccination (see *Variability in the Parameters of the Vaccination Model*). All other values that are not derived from the posterior are set to the parameter values in table 1 of Kaplan *et al*. (5) or to more conservative values favoring trace vaccination as described below in the section on *Variability in the Parameters of the Vaccination Model*.

Variability in the Parameters of the Vaccination Model

All vaccination parameters were set at Kaplan *et al.*'s (5) baseline rates except for p, the fraction of contacts named, which was conservatively set to 1.0. Also, we assumed that individuals in the early stages of the disease, specifically the first 27% of the latency stage prior to the outbreak of the fever, can be successfully vaccinated. Another difference is that Kaplan *et al.* (5) assume that the prodromal or fever period is infectious; because informed opinion suggests that it is not (6, 7), we instead assume that the prodromal period is noninfectious. Individuals in our model therefore are neither diagnosed as having smallpox nor automatically quarantined until they start exhibiting obvious signs of the disease. Because the early phases of smallpox can be easily confused with the symptoms of other infectious diseases (7), and because few currently practicing physicians have ever diagnosed smallpox, it is unclear how rapidly infected individuals could be diagnosed. We therefore varied the percentage of the infectious period that an infected individual could circulate between 23% and 38% of the overall infectious period. These values correspond to diagnosis at the macales stage, at which flat, discolored patches appear on the skin, and the pustules phase, at which blisters form (7).

Because some have argued that the vaccination rates in Kaplan *et al.* (5) are overly pessimistic, it was also important to consider more optimistic scenarios. We therefore considered two more optimistic vaccination scenarios, in addition to the scenario used in the main text, and reran the queuing model (5) for the case in which we allow for uncertainty in all parameters. Under a moderately optimistic scenario, we increased the number of traced social contacts from 50 to 300, and we increased the number of vaccinators from 5,000 to 10,000. As Fig. 9 shows, under this scenario, the median difference between the trace and mass vaccination strategies when using R_0 estimates based on Old World populations is reduced to 17,000, but there is still a substantial probability that the difference will be higher than 25,000. Similarly, for New World populations, the median difference between the two strategies is reduced to 181,000, but there is still a substantial probability that

the difference will be higher than 1 million. Under a wildly optimistic scenario, we increased the number of traced social contacts from 50 to 1.25 million, and the number of vaccinators from 5,000 to 125 million. As Fig. 10 shows, under this scenario, trace vaccination is more effective than mass vaccination when we use R_0 estimates based on Old World populations, because trace vaccination is virtually identical to mass vaccination. Nevertheless, when we use R_0 estimates based on New World populations, there is still a strong possibility that trace vaccination will produce 1 million or more additional deaths relative to mass vaccination, and uncertainty is still very high.

Absolute Number of Deaths Under Each Vaccination Strategy

For brevity, in the main text we show the effects of the two vaccination strategies in terms of the difference in the number of deaths between the two. In fact, the absolute number of deaths under mass vaccination is very small, especially compared to trace vaccination; moreover, most of the uncertainty in the difference in the number dead is due to uncertainty in the number dead under trace vaccination. To show this uncertainty, in Fig. 11, we show the distribution of the number of dead for both mass and trace vaccination when R_0 is estimated from Old World populations, and in Fig. 12, we show the corresponding distributions when R_0 is estimated from New World populations. As the figures show, almost all the variability in the difference in the number of dead between the two strategies is due to variability in the number of dead under trace vaccination.

Heterogeneity in Susceptibility: Impacts on $\mathrm{R_0}$ and Vaccination

As we describe in the main text, increasing model complexity by adding an additional parameter to account for heterogeneity in susceptibility among individuals had little effect on our results. As Table 1 shows, the 95% credible interval on $\bar{R}_0$, the equivalent of R_0 for the model with heterogeneity, has a reduced upper bound relative to the median for the model without heterogeneity, but the medians of the two distributions are nearly the same. This assumption suggests that the only meaningful change is a reduction in the tail of the distribution of $\bar{R}_0$; indeed, Fig. 13 shows that

Fig. 9. The difference in the number of deaths between the trace and mass vaccination scenarios for an optimistic vaccination scenario. (A) is for parameters based on Old-World populations, and (B) is for parameters based on New-World populations. Note differences in scales on the axes.

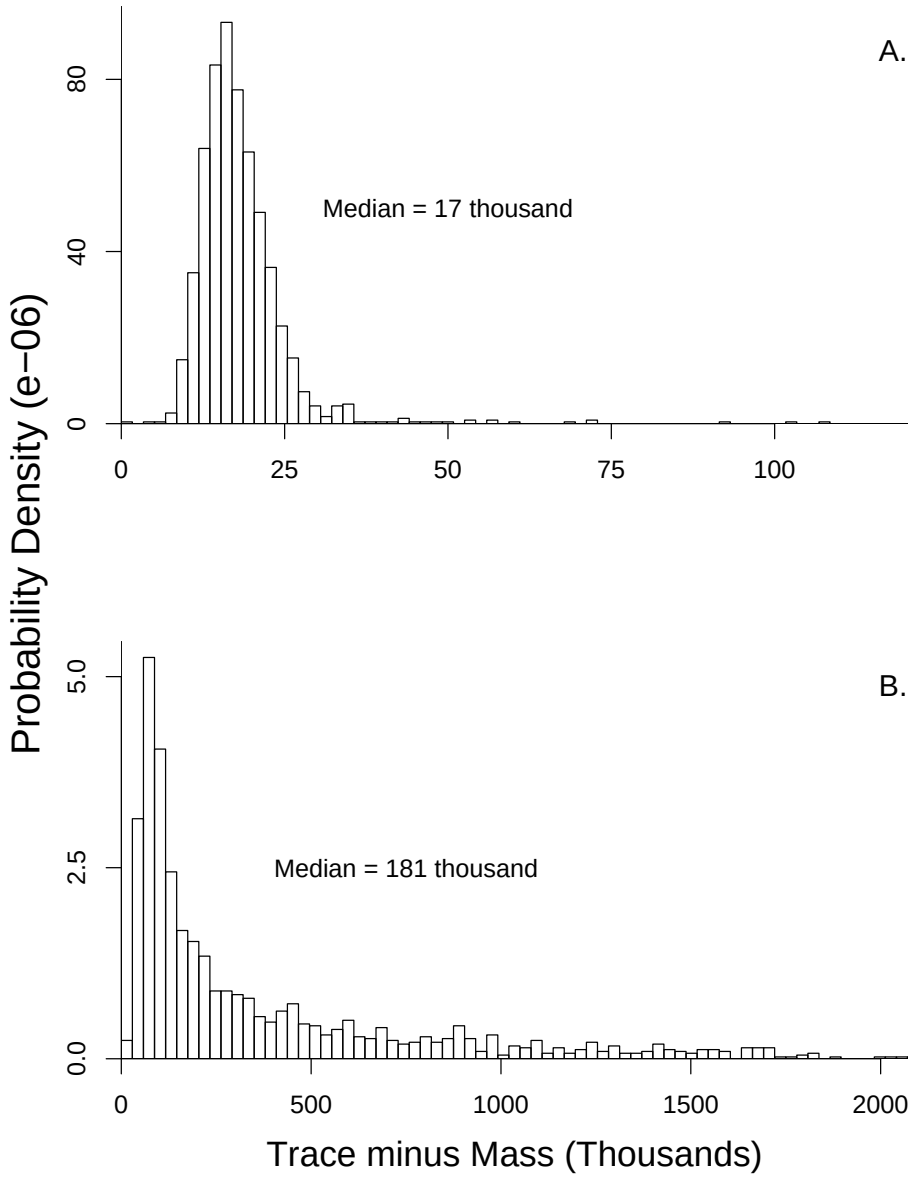

the two distributions are very similar for both the previously exposed Old World and previously unexposed New World populations. As a result, there is little or no change in the distribution of the difference in the number of dead under the two vaccination strategies, as shown by a comparison of Fig. 14 to Fig. 3.

Fig. 10. The difference in the number of deaths between the trace and mass vaccination scenarios for a wildly optimistic vaccination scenario. (A) is for parameters based on Old-World populations, and (B) is for parameters based on New-World populations. The gray line represents the division between trace and mass vaccination. Note differences in scales on the axes.

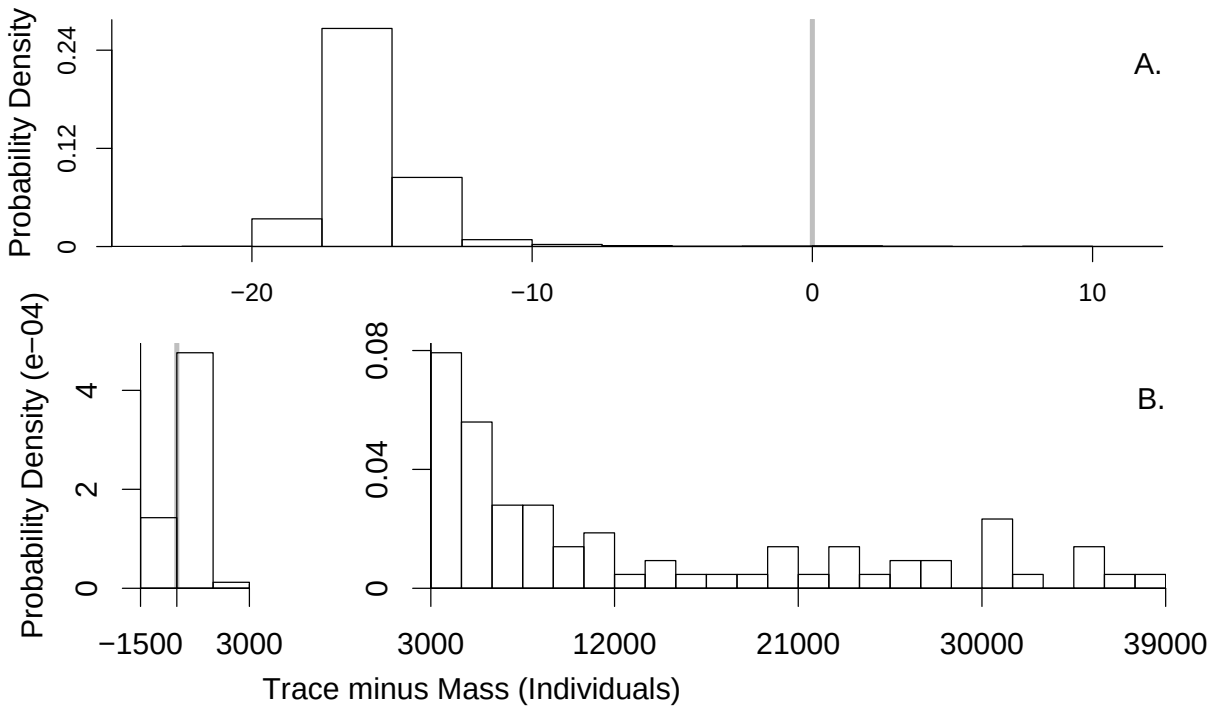

This lack of difference between the outcomes of the two models is further reflected in the overall number of deaths under mass and trace vaccination for both Old World and New World populations (Fig. 15 and Fig. 16 as compared to Fig. 11 and Fig. 12, respectively). Increasing the model's complexity thus has little effect on the uncertainty in the number of dead under the two strategies.

Fig. 11. The number of deaths in Old-World populations using (A) mass vaccination and (B) trace vaccination given an outbreak in a city of 10 million. The grey histogram in each panel shows the case in which we assume that there is no uncertainty in any SEIR model parameter except R_0 ("fixed"), while the black-outlined histogram shows the case in which we instead assume that all model parameters are uncertain, and we have integrated out all the other parameters ("variable"). Note differences in scales on the axes.

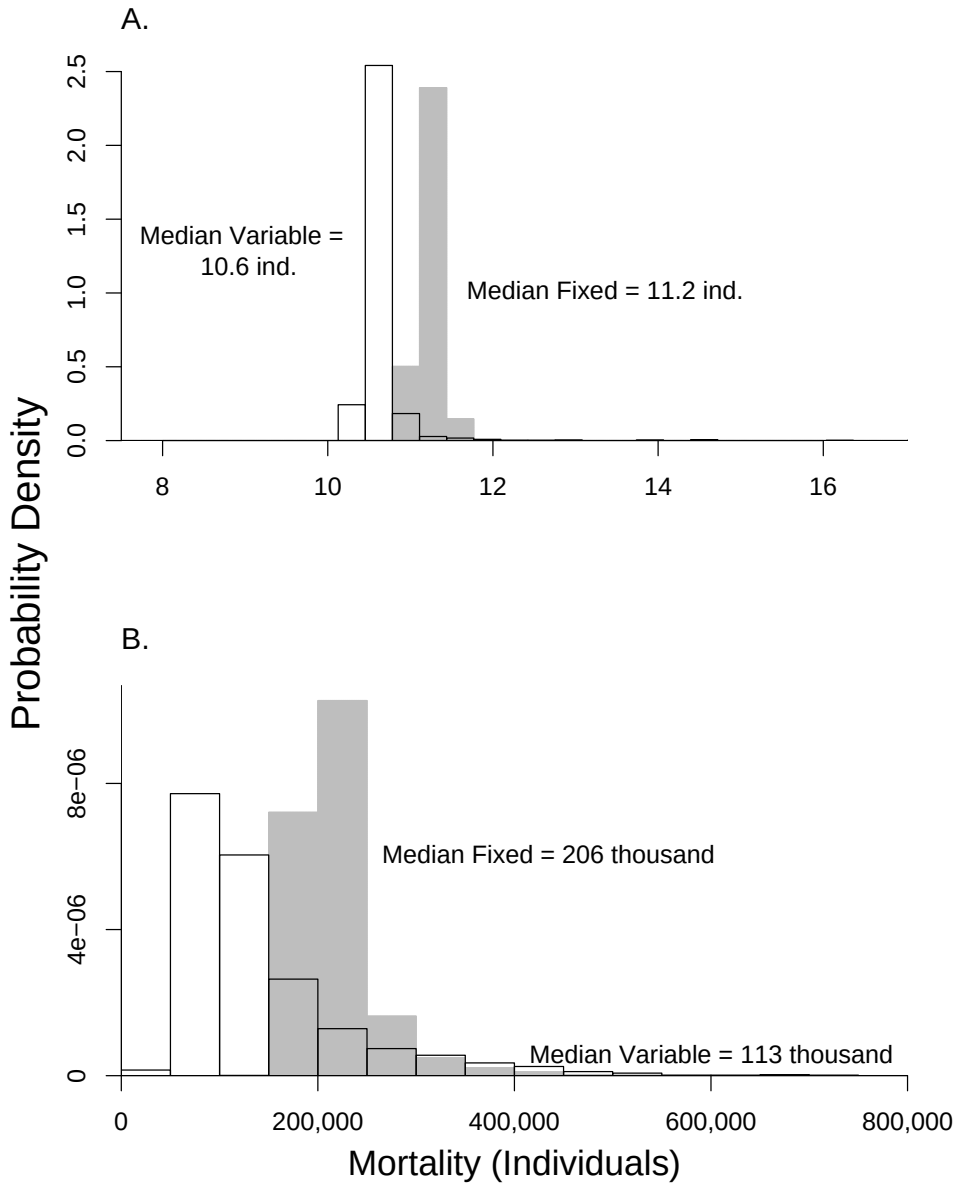

Fig. 12. The number of deaths in New-World populations using (A) mass vaccination and (B) trace vaccination given an outbreak in a city of 10 million. The grey histogram in each panel shows the case in which we assume that there is no uncertainty in any SEIR model parameter except R_0 ("fixed"), while the black-outlined histogram shows the case in which we instead assume that all model parameters are uncertain, and we have integrated out all the other parameters ("variable"). Note differences in scales on the axes.

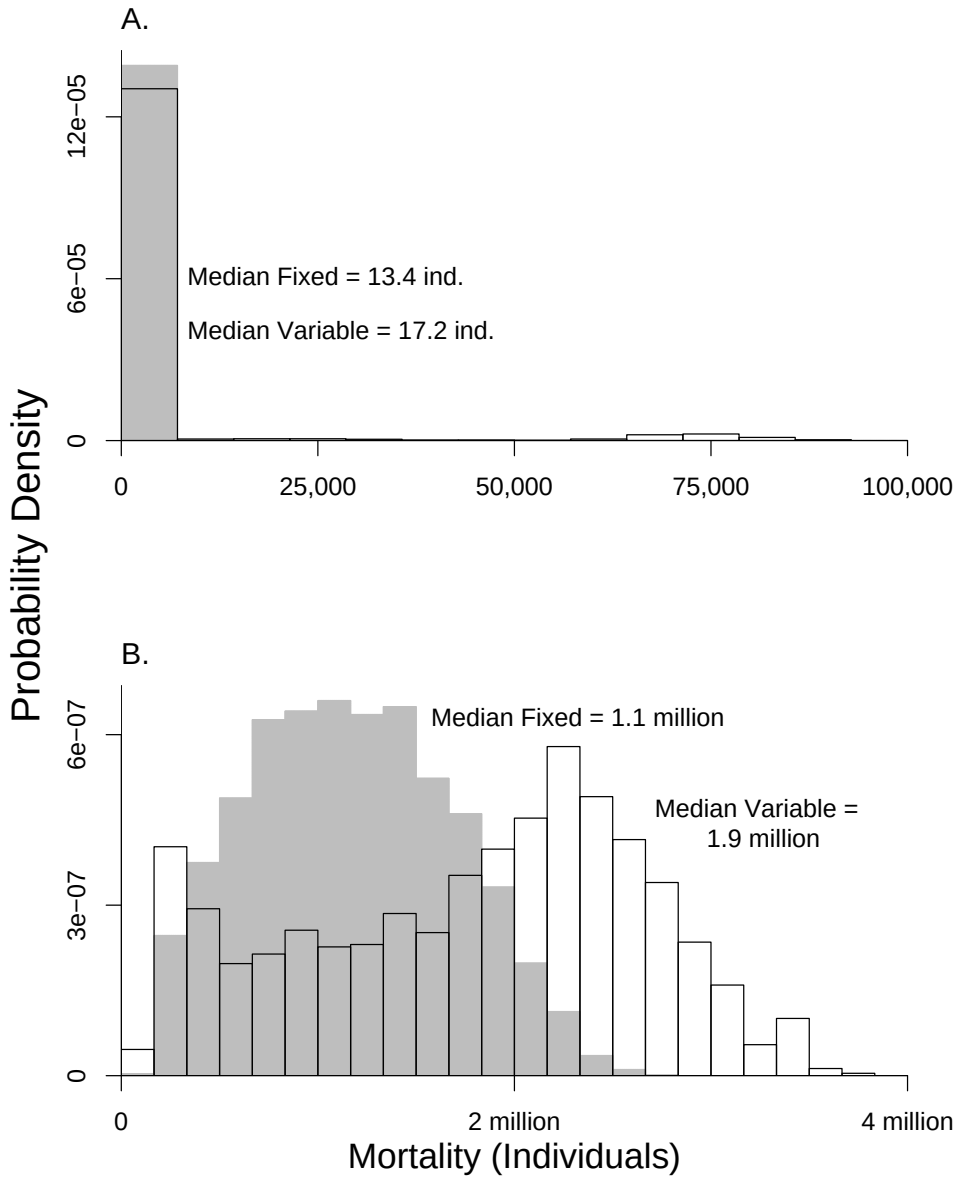

Fig. 13. Effects of prior knowledge on uncertainty in the disease transmission rate R_0 for the SEIR model and the heterogeneous SEIR model. The estimated posterior density of R_0 for Old-World (A) and New-World (B) populations are shown separately. The curved black line represents the prior distribution. The grey histogram in each panel shows the case in which we assume that there is no heterogeneity in susceptibility among individuals, while the black-outlined histogram shows the case in which we instead assume that there is heterogeneity in the population. Note differences in scales on the axes.

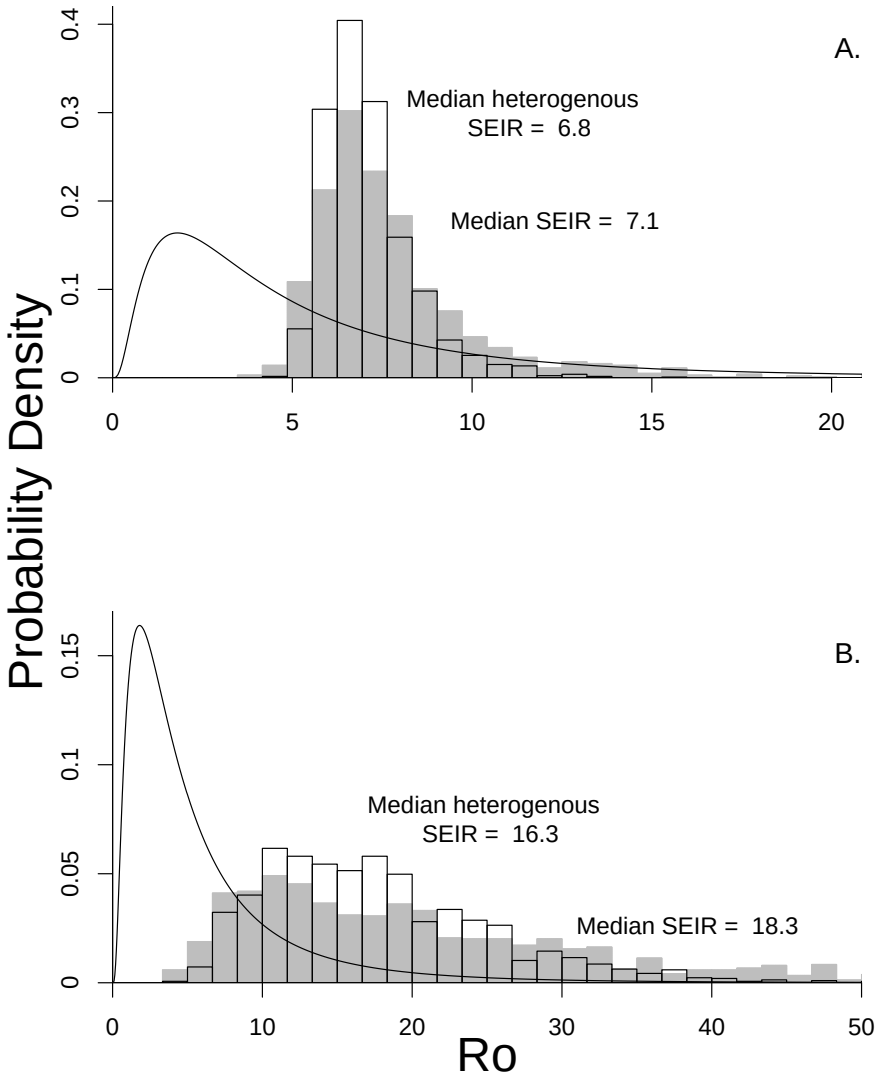

Fig. 14. Difference in the number of deaths between trace vaccination and mass vaccination strategies in a simulated population of 10 million: (A) Using parameters based on Old-World populations. (B) Using parameters based on New-World populations. Note differences in scales on the axes.

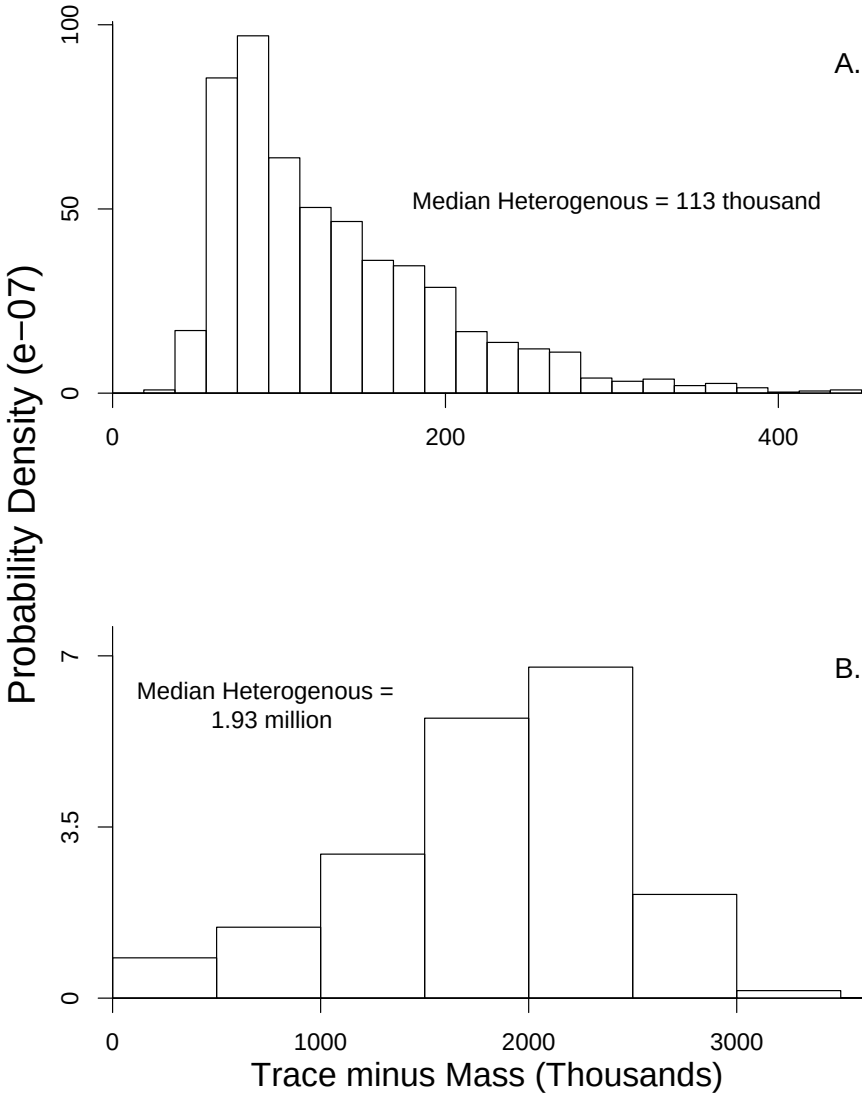

Fig. 15. The number of deaths in Old-World populations using (A) mass vaccination and (B) trace vaccination given an outbreak in a city of 10 million when assuming heterogeneity in susceptibility. Note differences in scales on the axes.

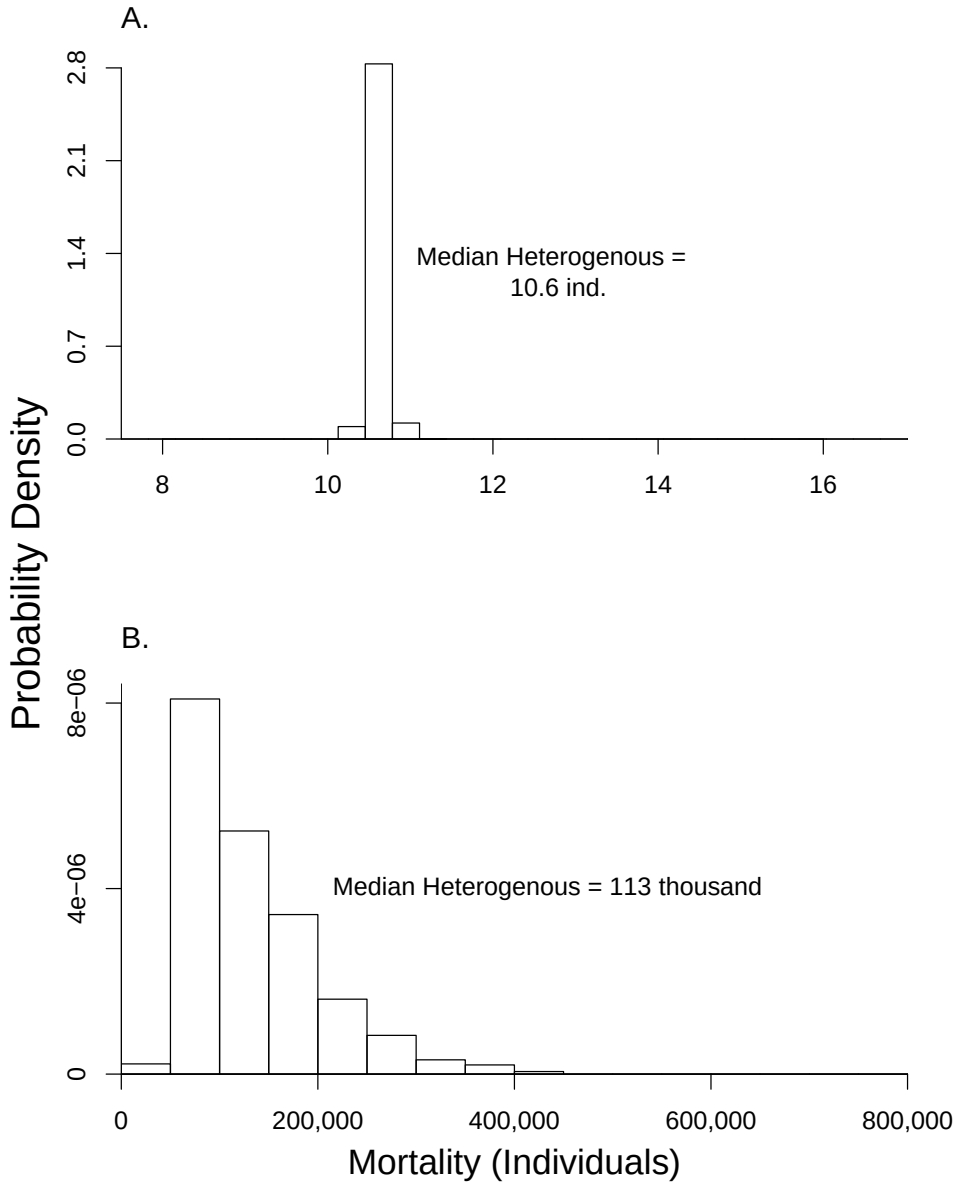

Fig. 16. The number of deaths in New-World populations using (A) mass vaccination and (B) trace vaccination given an outbreak in a city of 10 million when assuming heterogeneity in susceptibility. Note differences in scales on the axes.

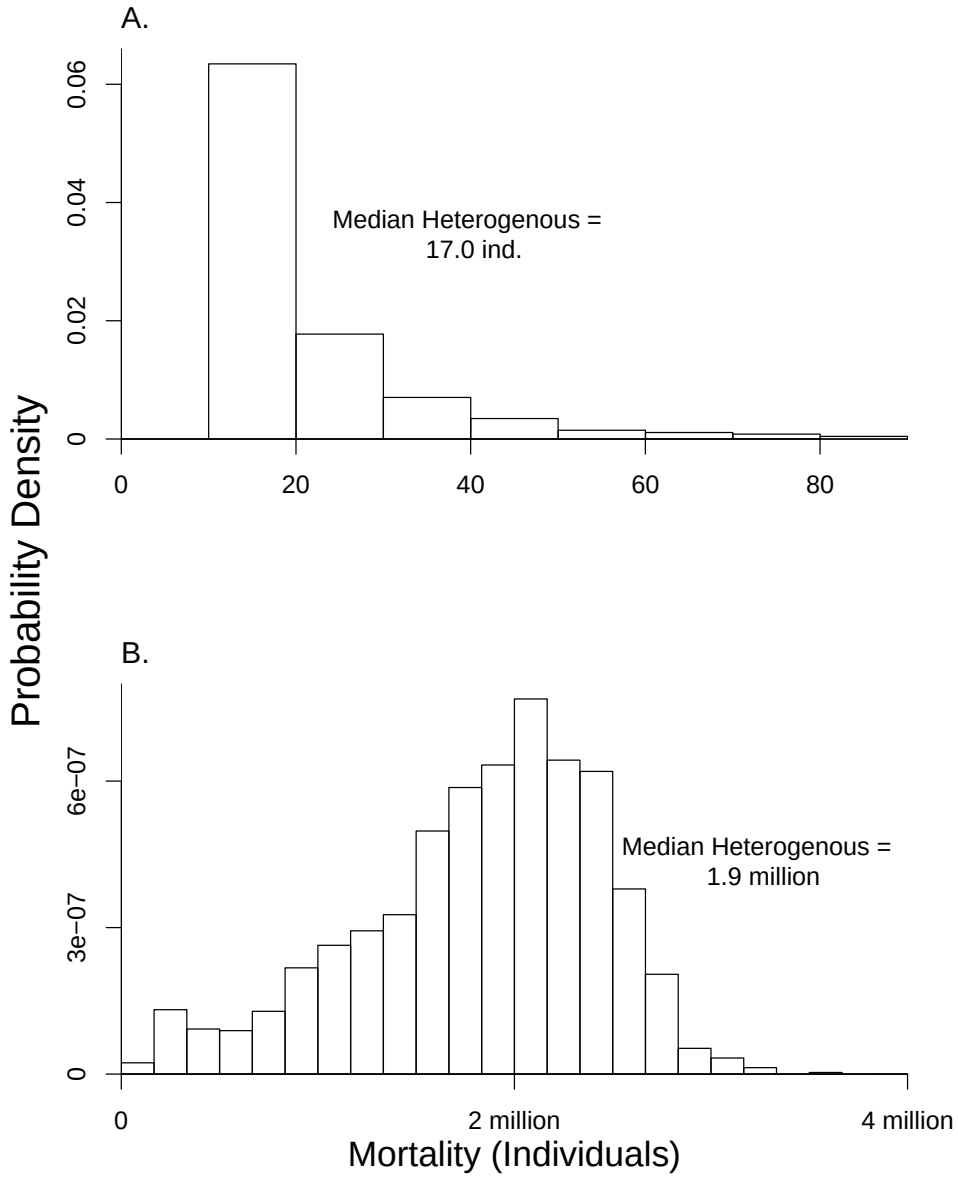

A Simple Method of Including Variability in Susceptibility in the SEIR Model

In order to model the effects of heterogeneity in a population's susceptibility, we used a moment-closure approach (8–10). Under the assumption that individuals vary in their susceptibility to the disease, the SEIR model becomes:

$$\begin{aligned} \frac{\partial S}{\partial t} &= -\frac{R_0\gamma}{N}SI, \\ \frac{dE}{dt} &= I\frac{\gamma}{N}\int_0^\infty R_0 S(R_0,t)dR_0 - \alpha E, \\ \frac{dI}{dt} &= \alpha E - \gamma I, \\ \frac{dR}{dt} &= \gamma I \ . \end{aligned} \tag{21}$$

The moment-closure method reduces the partial differential equation in Eq. **21** to a set of ordinary differential equations. First, we define:

$$S_j = \int_0^\infty {R_0}^j S(R_0,t)dR_0 \ , \tag{22}$$

where S_j is the jth moment of $S(R_0,t)$. By differentiating Eq. **22** with respect to time and substituting from Eq. **21**, we get:

$$\frac{dS_j}{dt} = -IS_{j+1} \ . \tag{23}$$

If we define $m_j \equiv S_j/S_0$ to be the jth moment of the frequency distribution of susceptibility, and differentiate m_j with respect to time, we have:

$$\frac{dm_j}{dt} = -I(m_{j+1} - m_j m_1) \ . \tag{24}$$

Recall that m_1 is the mean of the distribution of host susceptibilities. We therefore have replaced the partial differential equation in Eq. **21** with an infinite series of ordinary differential equations,

such that each moment is a function of a higher-order moment. To approximate the higher order moments and, thus, close the moments, we assume that the coefficient of variation remains constant. This finding turns out to be a reasonable approximation for most initial distributions of susceptibility (10). If k is defined as the inverse squared coefficient of variation then:

$$k = \frac{m_1^2}{m_2 - m_1^2} \quad . \tag{25}$$

Thus, by substituting Eq. **25** into Eq. **24** with respect to the first moment, we have:

$$\frac{dm_1}{dt} = -\frac{Im_1^2}{k} \quad . \tag{26}$$

Also note that Eq. **23** can be approximated with $j = 0$ as:

$$\frac{d\hat{S}}{dt} = m_1 I\hat{S} \quad . \tag{27}$$

We then divide Eq. **26** by Eq. **27**, integrate from 0 to t and solve for m:

$$m_1 = \frac{\bar{R}_0\gamma}{N}\left(\frac{\hat{S}(t)}{\hat{S}(0)}\right)^{1/k} \quad . \tag{28}$$

remembering that at time 0, $m(0)$ is the mean of the disease reproductive rate, $\bar{R}_0$. We now substitute Eq. **28** into Eq. **27** to derive an ordinary differential equation for the total population size $\hat{S}$;

$$\frac{d\hat{S}}{dt} = -\frac{\bar{R}_0\gamma}{N}\left(\frac{\hat{S}(t)}{\hat{S}(0)}\right)^{1/k} I\hat{S} \quad . \tag{29}$$

This gives the following set of ordinary differential equations:

$$\begin{aligned} \frac{dS}{dt} &= -\frac{\bar{R}_0\gamma}{N} SI\left(\frac{S(t)}{S(0)}\right)^{1/k}, \\ \frac{dE}{dt} &= \frac{\bar{R}_0\gamma}{N} SI\left(\frac{S(t)}{S(0)}\right)^{1/k} - \alpha E \ , \end{aligned} \tag{30}$$

where k is the inverse of the square root of the coefficient of variation of the distribution of R_0 across individual hosts. k is thus an inverse measure of the variability in susceptibility among individuals in the population. More susceptible individuals will acquire smallpox earlier in the outbreak (11). As the epidemic progresses, susceptibility of the noninfected decreases as R_0 is scaled by smaller and smaller values of $S(t)/S(0)$. The larger the value of k, the closer the model is to the homogeneous model (Eq. **1**) and models with values of $k > 200$ are nearly indistinguishable from models that assume all individuals are identical.

Note that, in numerically solving these and all other differential equations, we used an automatic second- and third-order pair step-size Runge-Kutta-Fehlberg integration method or a simple fourth- and fifth-order Runge-Kutta algorithm (Matlab; Mathworks, Natick, NA). In general, the SEIR equations (Eq. **1**) are well known for their numeric stability (i.e., the state variables change very smoothly over time) (11), and the use of both integration methods noted above perform well with such equations (12).

References

1. Bozzette, S. A., Boer, R., Bhatnagar, V., Brower, J. L., Keeler, E. B., Morton, S. C. & Stoto, M. A. (2003) *N. Engl. J. Med.* **348**, 416–425.

2. Gani, R. & Leach, S. (2001) *Nature* **414**, 748–751.

3. Efron, B. & Tibshirani, R. J. (1998) *An introduction to the boostrap* (Chapman and Hall, Boca Raton, FL).

4. Rigau-Pérez, J. G. (1982) *J. Hist. Med.* **37**, 423–438.

5. Kaplan, E. H., Craft, D. L. & Wein, L. M. (2002) *Proc. Natl. Acad. Sci. USA.* **99**, 10935–10940.

6. Eichner, M. & Dietz, K. (2003) *Am. J. Epidemiol.* **158**, 110–117.

7. Fenner, F., Henderson, D. A., Arita, I., Jezek, Z. & Ladnyi, I. D. (1998) *Smallpox and its eradication* (WHO, Geneva).

8. Dwyer, G., Elkinton, J. S. & Buonaccorsi, J. P. (1997) *Am. Nat.* **150**, 685–707.

9. Lloyd, A. (2004) *Theor. Popul. Biol.* **65**, 49–65.

10. Dushoff, J (1999) *Theor. Popul. Biol.* **56**, 325–335.

11. Anderson, R. M. & May, R. M. (1991) *Infectious Diseases of Humans: Dynamics and Control* (Oxford Univ. Press, Oxford).

12. Kreyszig, E. (1993) (Wiley).

The Sources of the Epidemic Data

Table 3. List of epidemics used in the smallpox outbreak models

Epidemic	Year	Population Size	Ref.
Boston	1721	10,565	1
Burford	1758	1,520	2
Chester	1774	12,009	1
Warrington	1773	7,000	1
Mauritius	1891	37,110	3
Saint Lawrence	1781	215	4*
Santo Domingo, New Mexico	1781	578	4*
Santa Clara	1780	627	4*
San Buenaventura	1780	501	4*
San Francisco Xavier	1780	261	4*
Rosalia	1781	133	4*
Pojoaque	1781	270	4*
Santo Domingo, Baja California	1781	119	4*

* Population sizes of initially susceptible individuals derived from the census of 1777 (5) and 1778 (6). Forecasting of population size up to the time of the epidemic was carried out using background birth and death rates from various sources (6–9).

References for Table 3

1. Creighton, C. (1891) *A History of Epidemics in Britain* (Cambridge Univ. Press, Cambridge, UK), Vol 2.

2. Moody, J. (1997) *The Great Burford Small-Pox Outbreak* (HindSight of Burford, Oxfordshire, UK).

3. Anderson, D. E. (1918) *The Epidemics of Mauritius* (Lewis, London).

4. Fenn, E. A. (1999), Dissertation, (Yale University, New Haven, CT).

5. Adams, E. B. & Chavez, F. A. (1956) *The Missions of New Mexico, 1776: A Description by Fray Francisco Atanasio Dominguez with Other Contemporary Documents* (University of New Mexico Press, Albuquerque).

6. Archivo General de Indias, Sección Indiferente General (1778) *Padrones de Cusiguríachic* (Archivo General de Indias, Sección Indiferente General, Cusiguríachic, Mexico).

7. Jackson, R. H. (1983) *J. Calif. Great Basin Anthropol.* **5**, 131–139.

8. Jackson, R. H. (1981) *J. Calif. Great Basin Anthropol.* **3**, 138–143.

9. Jackson, R.H. (1994) *Indian Population Decline: The Missions of Northwestern New Spain, 1687-1840* (University of New Mexico Press, Albuquerque).